



Journal of Mining and Environment (JME)

journal homepage: www.jme.shahroodut.ac.ir



Rock Joint Micro-Scale Surface Roughness Characterisation using Photogrammetry Method

Mojtaba Bahaaddini^{1, 2*}, Mehdi Serati³, Mohammad Hossein Khosravi¹ and Bruce Hebblewhite⁴

1. School of Mining Engineering, College of Engineering, University of Tehran, Tehran, Iran

2. Shahid Bahonar University of Kerman, Kerman, Iran

3. School of Civil Engineering, The University of Queensland, Brisbane, Australia

4. School of Minerals and Energy Resources Engineering, UNSW Sydney, Sydney, Australia

Article Info

Received 15 February 2022

Received in Revised form 25 February 2022

Accepted 28 February 2022

Published online 28 February 2022

DOI: [10.22044/jme.2022.11669.2155](https://doi.org/10.22044/jme.2022.11669.2155)

Keywords

Rock joint

Joint surface roughness

Shear behaviour

Photogrammetry

Laser scanner

Abstract

A proper understanding of the shear behaviour of rock joints and discontinuities is yet a remaining challenge in the rock engineering research works owing to the difficulties in quantitatively describing the joint surface roughness both at the field and the laboratory scales. Several instruments and techniques have been developed over the years for the surface characterisation of joints at the field- and laboratory-scale investigations, amongst which the application of the photogrammetry methods has obtained a growing popularity. This work evaluates the applicability of the photogrammetry techniques for the characterisation of joint surface topography and texture at micro-scales, which has been largely understudied in the literature. Three tensile joint surfaces are digitized using photogrammetry, and the results are compared with those obtained from laser scans with a high 3D accuracy. A comprehensive statistical analysis is then undertaken on the digitized point clouds in order to assess the performance of photogrammetry in surface characterisation. The results of this work show that the height differences between the resulting point clouds from the two adopted techniques (photogrammetry and 3D laser scanning) follow the normal distribution with the mean values close to zero. The statistical analyses illustrate that the measured joint surfaces using the photogrammetry techniques are in good agreement with the laser scanning data, confirming that photogrammetry is a capable method for characterising the joint surface roughness even at micro-scales. Interestingly, the results obtained further indicate that the accuracy and preciseness of the photogrammetry techniques are independent from the joint roughness coefficient but the camera and configuration parameters remarkably control the performance of the measurement.

1. Introduction

Rock mass behaviour near underground openings as well as at shallow depths can be significantly influenced by the presence of discontinuities. The mechanical behaviour of discontinuities such as the shear strength is a paramount factor in the development of a mine when safety is the main concern. The joint surface roughness has been widely known to be one of the main parameters controlling the hydraulic and shear behaviour of rock joints. A large number of studies have been

carried out in the last five decades in order to provide the analytical and empirical models to predict the shear behaviour of rough rock joints [1-7]. Despite such successful efforts, quantifying the contribution of joint surface roughness to the shear behaviour of rock joints (with accuracy and ease) yet remains a challenging task in geotechnical engineering. This limitation is believed to be predominantly related to the lack of a unique and widely accepted method for quantitatively

✉ Corresponding author: m.bahaaddini@ut.ac.ir (M. Bahaaddini).

describing the complex geometry of a joint surface and unknown contribution of different order asperities involvement in the shearing process [8-11]. Numerous empirical, statistical, and fractal methods have been proposed in the recent years to present the joint surface roughness using a quantitative value [4, 12-14]. Amongst many available techniques, the recent developments in photogrammetry have provided a fast, simple, and cost-efficient solution for digitising rock surface textures. Nevertheless, more research has been deemed necessary to assess the applicability of the photogrammetry methods in characterising joint surface textures at the micro and grain scales; that this work is aimed to deliver. In this work, first, the conventional approaches for the characterisation of joint surfaces are discussed, and laser scanning is preferred as a benchmark point. The surface textures of three different tensile joints were then characterized using the photogrammetry techniques and compared with those resulting from the benchmark results. A comprehensive statistical analysis (based on different approaches such as Bland-Altman analysis and cumulative frequency of the prediction error) was finally conducted on the quantified joint surface point clouds obtained from both the photogrammetry and laser scanning techniques.

2. Surface characterisation of discontinuities

A precise measurement of joint surface roughness is a crucial step in the study of shearing mechanisms and estimation of the shear strength and dilation behaviour of rock joints. Various instruments and techniques have been developed and utilized in order to quantify the rock joint surface topography in the laboratory or field conditions. Each method has its advantages and limitations; hence, selection of the most appropriate technique depends on several factors including size or scale of the study, measurement speed, precision, repeatability, spatial resolution, easiness in measurement and data analysis, applicability to field condition, and cost. These methods can be divided into two main categories, namely, contact and non-contact methods reflecting whether direct contact with the rock joint surface is required during the measurement process.

2.1. Contact methods

Contact methods can be sub-categorised into (i) linear profiling and (ii) local surface orientation approaches, which are essentially 2D and 3D

methods in nature, respectively. In the linear profiling method, the perpendicular distances from a reference line to the joint surface at regular distances is measured using a physical measurement instrument. Profile comb [4], stylus and roller profilometers [15], straight edges and rulers [16], and shadow profilometry [17, 18] are typical instruments used for linear profiling. Among these instruments, the mechanical or electrical stylus profilometers provide more precise digitized profiles [19], while their resolution depends on the dimension of the stylus (0.5–2 mm). It is worth noting that if the stylus contact point is spherical, the curvature of the surveyed points can be overestimated [20]. The applied load on the contact area can be another source of error. In this method, the digitisation of large surfaces is particularly time-consuming and difficult, making the method impractical and expensive. The compass and disc-clinometer [21], as well as the equilateral tripod and connecting pin sampling techniques [22], are two examples of the local surface orientation methods. These methods are based on the measurement of the local orientation of discs or the equilateral tripod and connecting pin devices that are in contact with the discontinuity surface.

2.2. Non-contact methods

The aforementioned contact methods have several drawbacks. They require access to the joint surface, which can be problematic for hazardous or non-accessible areas. In addition, the measurement of a large area is time-consuming and prone to errors due to sampling difficulties, human bias, and limitation of the instruments [23, 24]. In order to overcome these limitations, several non-contact measurement techniques have further been developed. The non-contact methods that are conventionally used in rock engineering can be sub-categorized into two main groups, namely passive and active triangulation (such as photogrammetry and structured light techniques) and direct and indirect measurement of distance (e.g. laser ranging) [25]. In the recent years, passive photogrammetry and laser-based distance measurement techniques are more commonly used for 3D mapping of rock structures. Over the past decade, significant developments have occurred in these two techniques, mainly in data acquisition and the effective integration of data into a known spatial reference system. The development of powerful computational resources has significantly supported these techniques. It is noted that these

techniques can be used at both the field and laboratory scales.

2.2.1. Laser ranging

In this method, the distance is measured directly based on the speed of light. A pulsed beam of light is emitted onto the object, and the required return travel time to the emission source after reflection from the surface is used for estimation of the relative distance. The direct acquisition of spatial data reduces the complexity of 3D surveying. In addition, the amount of computational analysis that is required to provide spatial data is also relatively lower compared to the passive triangulation methods such as photogrammetry. However, it requires precise positioning and orientation of the laser system. Such a technique also requires a longer set-up time in the field. It is worth mentioning that one of the important limitations of this technique is that the dark layers on the rock surface do not reflect the light, and no data can be captured using light-laser scanning [26].

2.2.2. Photogrammetry

Photogrammetry is the science of measuring the 3D spatial data from two or more 2D images taken from the same scene. The principle of such a technique is illustrated in Figure 1. The light that hits a given pixel in an image can come from any point along the ray from the pixel, through the perspective centre, into the scene (Figure 1a). By adding another image taken from a different location and projecting rays into the scene from each common point in both images through the perspective centre of the camera, the 3D location of the point can be determined (Figure 1b). Therefore, by pairing images of the same surface taken from different locations, the 3D spatial coordinates of a rock surface can be characterised (Figure 1c). The application of photogrammetry had been limited in the past due to the difficulty of automating the computational process to extract the 3D data, required time for computation, and issues related to film-based cameras. In the recent years, these limitations have been largely resolved by the development of digital photography and high-speed computers [25]. The main advantages of photogrammetry over the other techniques for

rock joint surface characterisation are its simplicity and the fast data generation process. Such an approach requires only two components including a digital camera and a computer where both are readily available at a relatively low cost [27]. The photogrammetry technique has also been successfully used in different large-scale mining and civil related projects including 3D spatial modelling in open-pit mines [27, 28], rock slope characterisation [23, 24, 29-31], structural mapping [24, 32-34], bench face surveying and designing blasting pattern [24], tunnel-face mapping, and underground structures performance [24, 35] as well as monitoring the strain rate and displacement in the geotechnical physical modelling projects such as retaining wall models [36-38] and soil slopes [39, 40]. However, the applicability of this technique for the characterisation of micro-scale asperities of rock joints has not yet been investigated in detail, and require further improvements.

3. Experimental methodology

In this work, three tensile joint surfaces were prepared from slabbed shape blocks of Hawkesbury sandstone. Hawkesbury sandstone dominates the Sydney basin, New South Wales, Australia—more details regarding the geo-mechanical properties of Hawkesbury sandstone can be found in [41-44]. In order to investigate, the results are not restricted to a specific joint texture; three joint surfaces having different surface morphology of slightly rough to very rough were prepared. The prepared samples are shown in Figure 2. The dimensions of joint surfaces were approximately 100 mm × 100 mm. The joint surfaces were digitized using both close-range photogrammetry and 3D laser scanner, and the results obtained were then compared. Using the 3D laser scanning point clouds and providing 2D profiles with a sampling interval of 0.5 mm, the joint roughness coefficient (*JRC*) of each sample was calculated using the roughness parameter of Z_2 [45, 46]. The results obtained showed that sample No. 3 had the greatest roughness value with $JRC = 17.3$, while those of samples No. 1 and No. 2 were $JRC_{Sample\ No.1} = 13.2$ and $JRC_{Sample\ No.2} = 12.5$, respectively.

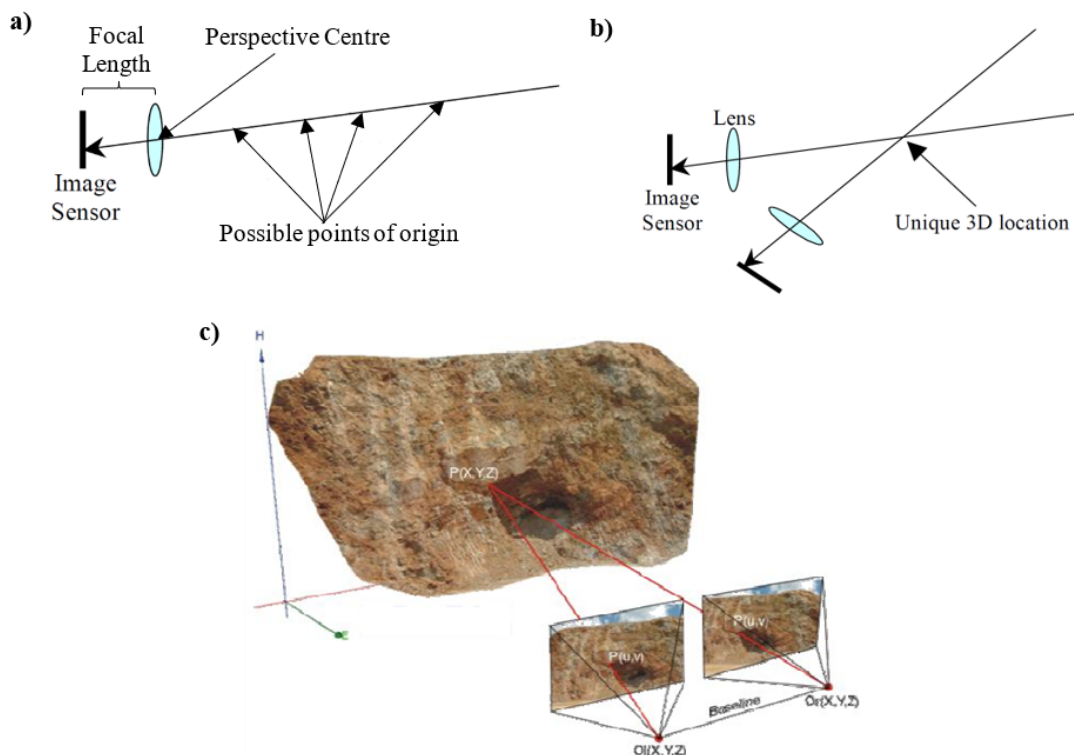


Figure 1. Principle of photogrammetry: (a) Problem of finding a unique 3D location using a single image, (b) Finding the unique 3D location through intersection of rays projected from two images, and (c) Process of finding 3D spatial data of rock surface from two 2D images [24, 27].



Figure 2. Three tensile joint surfaces of Hawkesbury sandstone having different joint roughness coefficient (JRC) values ($JRC_{Sample\ No.\ 1} = 13.2$, $JRC_{Sample\ No.\ 2} = 12.5$, and $JRC_{Sample\ No.\ 3} = 17.3$).

3.1. 3D laser scanning

FARO Laser ScanArm was used to digitize the joint surfaces based on the laser scanning technique. A common problem in laser scanning of rock joint surfaces is the possibility of missing some surface points due to rapid variations in the roughness of asperities. The FARO Laser ScanArm is a 7-axis measurement device with a fully integrated laser line probe. FARO Laser ScanArm can overcome the issue associated with the potential of overlooking some surface points as it can emit the laser beam in different directions. Such a device can digitize 19,200 points per second with a high accuracy ($\pm 50\ \mu\text{m}$). The process of

digitising a joint surface using FARO Laser ScanArm and the resulting 3D joint surface is illustrated in Figure 3. A local coordinate system has been assigned for this equipment, and the laser source originates from this coordinate system in parallel to the Z-axis. The FaroArm performs as a localiser and tracks the position of the laser line probe coordinate systems in space, and then transform it into the FaroArm coordinates. The single point repeatability of the system presents the ability to record identical results after measuring the same fixed point in space. Several factors may affect the accuracy of the ScanArm. Due to the optical nature of the device, the parameters such as

closeness to the scan subject, humidity, temperature, and surface features like, color, texture, and reflectivity may attribute the scan performance. A built-in functionality of the FaroArm reduces the noise of reflective surfaces and optics and software algorithms minimise the speckling effects. The laser line probe performance is expressed based on the entire field of view. Scanning of far fields improves the scan width

through fewer laser passes with reduced accuracy, while scanning of near fields improves the accuracy with reduced effective scan width. Therefore, the optimum location should be specified in the middle field for best performance and scan coverage. The scanned data from the FARO Laser ScanArm system was interpreted by the PolyWorks software to generate the 3D digitized datasets.

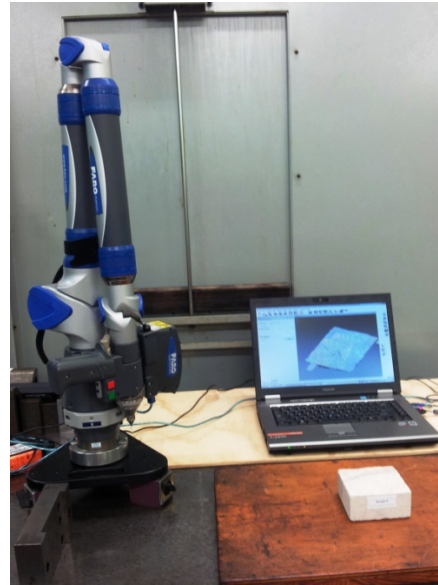


Figure 3. Digitising a typical joint surface using FARO Laser ScanArm.

3.2. Digitising joint surface using photogrammetry

The step-by-step process of digitising joint surfaces using the photogrammetry method is illustrated in Figure 4. The first and essential step in photogrammetry, which must be undertaken before taking pictures, is the camera calibration (interior orientation). By calibrating the camera and lens, the locations of points in the image can be determined with the accuracy of up to one-tenth of a pixel, while distortion of the lens may result in the apparent locations being shifted internally dozen of pixels [47]. The calibration parameters include focal length (C), radial lens distortion (K_1, K_2, K_3, K_4), principal point offset in x and y directions (X_p, Y_p), decentring distortion (P_1, P_2), and scaling factors (B_1 and B_2). A Canon EOS5D mark II camera was used in this work. The camera calibration was undertaken using the 3DM CalibCam software (from ADAM Technology). The readers are referred to the 3DM Analyst Manual [47] for detailed information about the procedure of camera calibration.

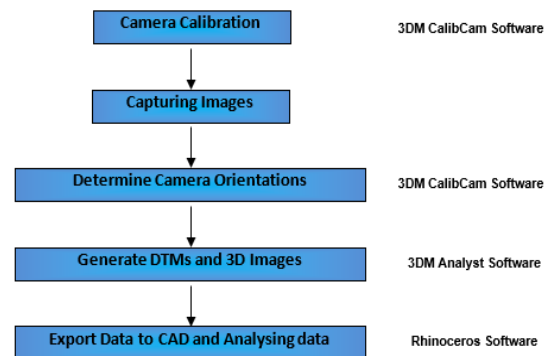


Figure 4. Step-by-step process of digitising joint surface using photogrammetry.

In the next step, several photos were taken from the joint surface at different locations. As shown in Figure 5a, two LED-based lighting systems were used to provide an even light illumination with minimal shadowing at the joint surface. In order to generate the 3D image, the precise location and orientation of the camera when each image is captured (the exterior orientation) must be known. In order to determine the exterior orientation, the 3DM CalibCam software was used, which used the

least squares bundle block adjustment algorithm [47]. In order to obtain correctly the scaled results, a few control points were selected on the joint surface. By knowing the distances between these points, the 3DM CalibCam was able to scale the model correctly. The relative-only points were then automatically generated by the 3DM CalibCam in order to establish the relationship between the camera positions with respect to each other. After

determination of the camera orientations, common points for each pair of images were identified to project rays into the scene leading to the determination of 3D coordinates of the captured points. Using the 3DM Analyst, 3D images and digital terrain models (DTM) were generated (Figures 5b and 5c). DTM of joint surfaces were saved as DXF files, and imported into the Rhinoceros software for further analysis.

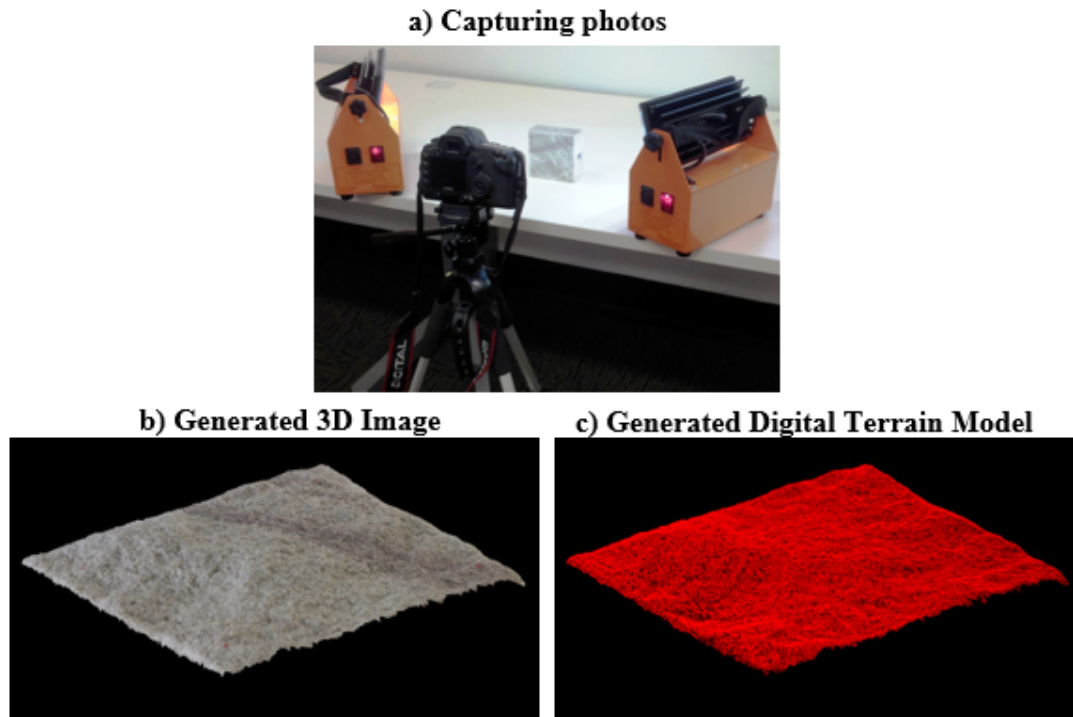


Figure 5. Capturing images and generating 3D data of joint surface of sample No. 3: (a) Taking photos of joint surface from different standpoints (b) Generated 3D image, and (c) Generated DTM.

4. Results and discussion

4.1. Statistical analysis

The results from both the laser scanning and photogrammetry techniques were compared to investigate the capability of photogrammetry in the characterisation of micro-scale roughness. Both 3D surfaces were imported into the Rhinoceros solids modelling software. The generated joint surfaces from both techniques for sample No. 2 are

presented in Figure 6. These surfaces were sliced into profiles, and then these profiles were digitized. The relative height difference between the digitized points of locations with the same coordinates of x and y presents the deviation between the laser scanning (Z_{Laser}) and photogrammetry ($Z_{Photogrammetry}$). Therefore:

$$\text{Height Difference} = Z_{Laser} - Z_{Photogrammetry} \quad (1)$$

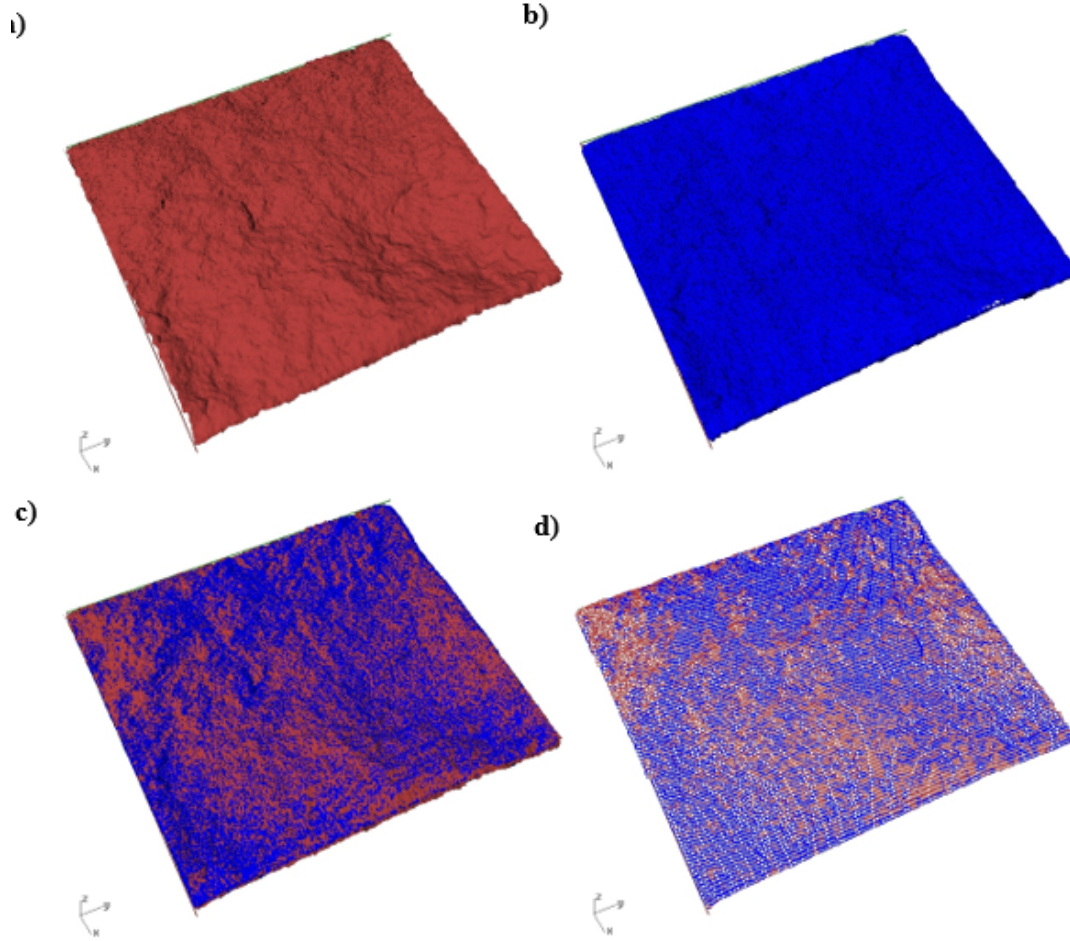


Figure 6. Comparison between generated joint surfaces for sample No. 2: (a) Photogrammetry (b) Laser scanning (c) Comparison between 3D surfaces, and (d) Digitised point clouds.

In order to statistically evaluate the suitability of photogrammetry for digitising the joint surface textures, the histograms of height differences for three samples were calculated, as shown in Figure 7. For all three samples, the height differences obey the normal distribution with the mean value close to zero.

The performance of the photogrammetry in the measurement of surface texture was firstly evaluated using the statistical parameters of root

mean square error (*RMSE*), the variance accounted for (*VAF*), and the coefficient of determination (R^2), as summarised below:

$$RMSE = \sqrt{\frac{1}{N} \sum (Z_{Laser} - Z_{Photogrammetry})^2} \quad (2)$$

$$VAF = \left(1 - \frac{var(Z_{Laser} - Z_{Photogrammetry})}{var(Z_{Laser})}\right) \times 100 \quad (3)$$

$$R^2 = 100 \times \left\{ \frac{\sum (Z_{Photogrammetry} - \bar{Z}_{Photogrammetry})(Z_{Laser} - \bar{Z}_{Laser})}{\sqrt{\sum (Z_{Photogrammetry} - \bar{Z}_{Photogrammetry})^2 \sum (Z_{Laser} - \bar{Z}_{Laser})^2}} \right\}^2 \quad (4)$$

where N is the number of data points and $\bar{Z}_{Photogrammetry}$ and \bar{Z}_{Laser} are the mean height of photogrammetry and laser scanning values, respectively. The mean difference can be representative of the bias (the systematic difference

between two methods), and the standard deviation of the differences (*SD*) can be representative of the precision (the random fluctuations around the mean). *RMSE* indicates both the bias and precision and low *RMSE* indicates high predictive ability.

VAF and R^2 are measures of preciseness and the one with a value close to 100% denotes high preciseness performance for a given dataset [48]. The results of the preliminary statistical analyses are presented in Table 1. These results show that for all three samples, the measured texture of joint

surface using photogrammetry is in good agreement with the laser scanning ones. It is noteworthy that based on the statistical parameters of RMSE, VAF and R^2 , the measurement performance in sample No. 2 seems better despite the highest mean height difference.

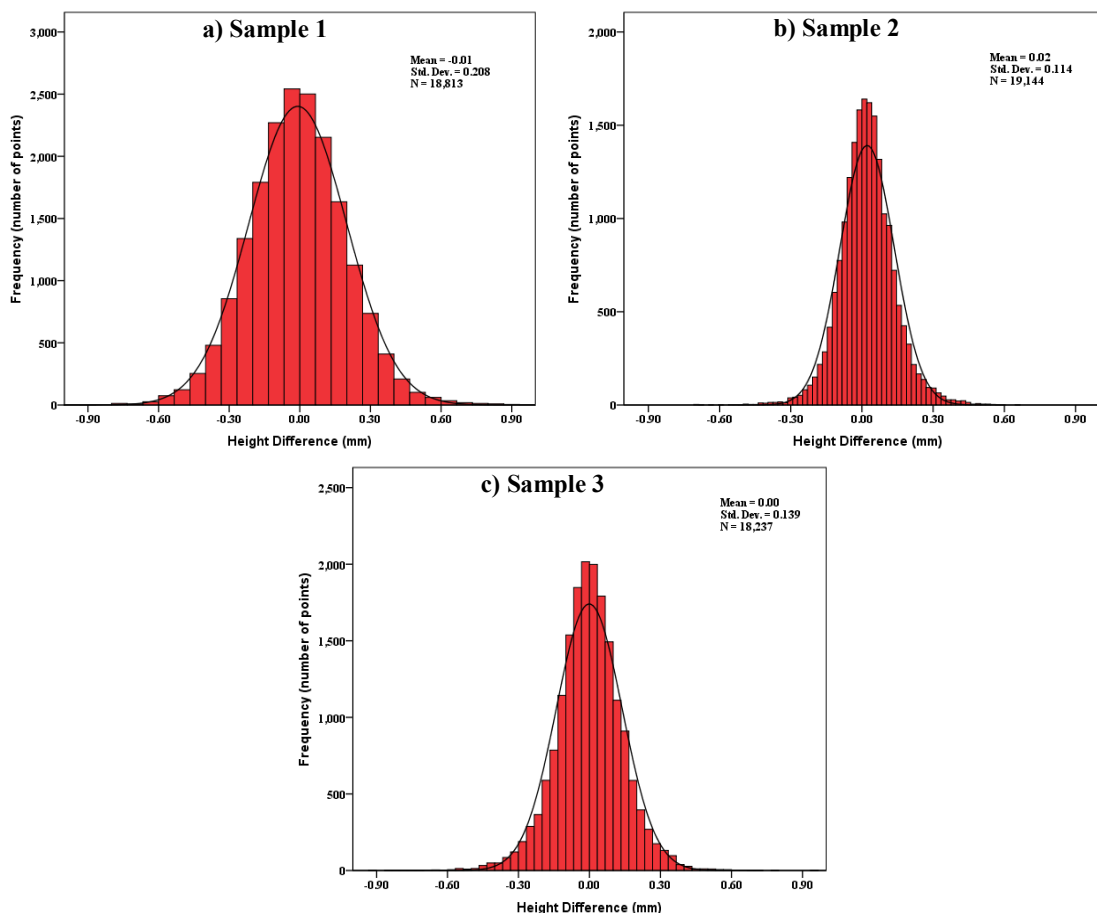


Figure 7. Distribution of height difference of digitized points using laser scanning and photogrammetry methods: a) Sample No. 1, b) Sample No. 2, and c) Sample No. 3.

Table 1. Results of preliminary statistical analyses.

Statistic	N	Mean (mm)	Standard Deviation (mm)	RMSE	VAF (%)	R^2 (%)
Sample 1	18,813	0.009	0.208	0.208	98.26	98.32
Sample 2	19,144	0.022	0.114	0.116	99.30	99.32
Sample 3	18,237	-0.001	0.139	0.139	99.32	99.32

As both methods of laser scanning and photogrammetry have a certain amount of measurement error, attempts were made to investigate whether these methods were comparable and whether the measurements results were sufficiently close to each other. To this end, the correlation between laser scanning and photogrammetry measured texture heights were

investigated and depicted in Figure 8. The results for all three samples show that the datasets are nearly concentrated close to the line of equality. As the data points tend to be clustered along the line of equality for large datasets in the plot of one method versus the other method [49], the analysis was followed by the Bland–Altman analysis.

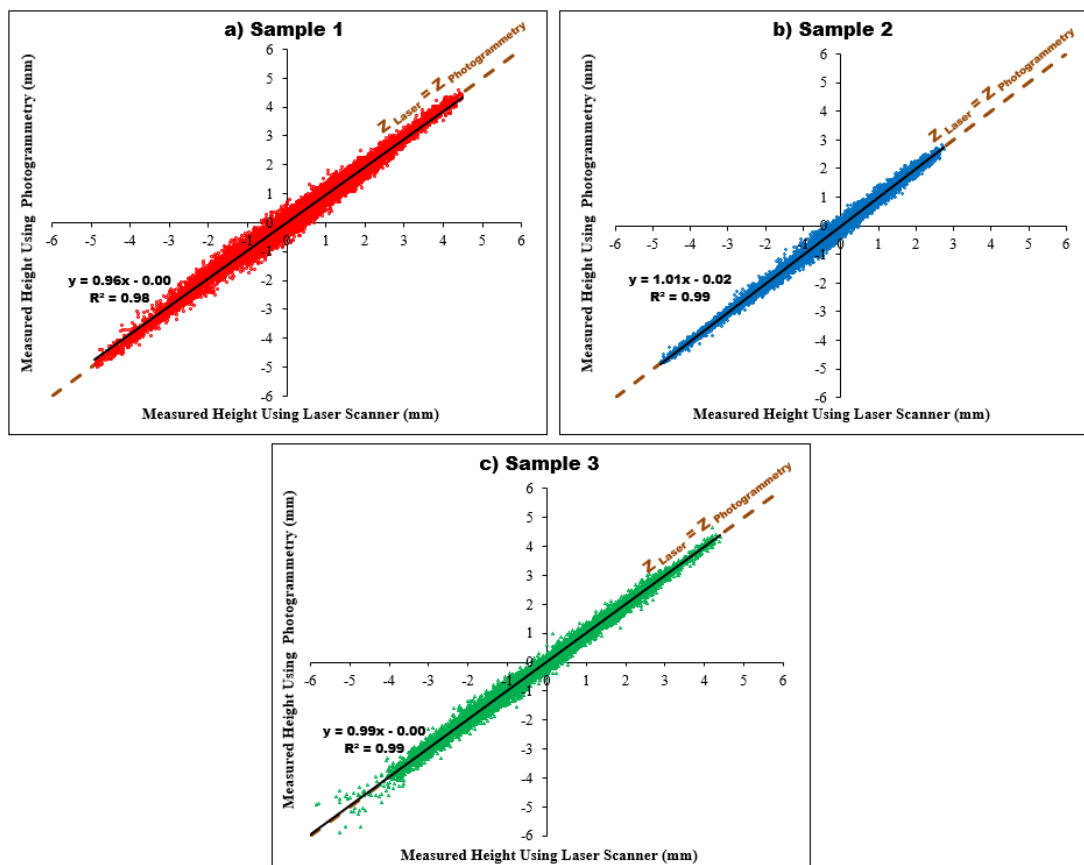


Figure 8. Measured heights using laser scanner versus photogrammetry for: a) Sample No. 1, b) Sample No. 2, and c) Sample No. 3.

The Bland-Altman analysis evaluates the agreement between the two techniques, and it can assess the interchangeability between a specific measurement technique compared to the reference one [49-51]. The mean difference between the measurement technique and the reference technique is a measure of accuracy (bias). The 95% limits of agreement (*LOA*) are used as a measure of precision, calculated as:

$$LOA = (Bias) \pm t_{\alpha, N-1} \cdot SD \quad (5)$$

where $t_{\alpha, N-1}$ is the *t*-value corresponding to the degree of freedom $N-1$ and significance level α [52]. The resulting graph of the Bland-Altman analysis is a scatter plot, where the difference of the two measurements is plotted versus the mean of the two measurements, as shown in Figure 9 for 95%

limit of agreement. The regression lines of difference on average values were plotted in order to evaluate the variability of measurement as the magnitude of the measurement (asperity height) increases. The regression lines can also be representative of a trend in the bias; in other words, a tendency for the mean difference to increase or decrease with an increment in the magnitude [50]. In sample No. 1, a slight increase in bias with increasing the magnitude is observed (positive slope of the regression line), while this trend cannot be observed in other samples. Therefore, the results of the Bland-Altman analysis show that the measured joint surface textures using the photogrammetry technique are in good agreement with the laser scanning results with a high accuracy and an acceptable range of preciseness.

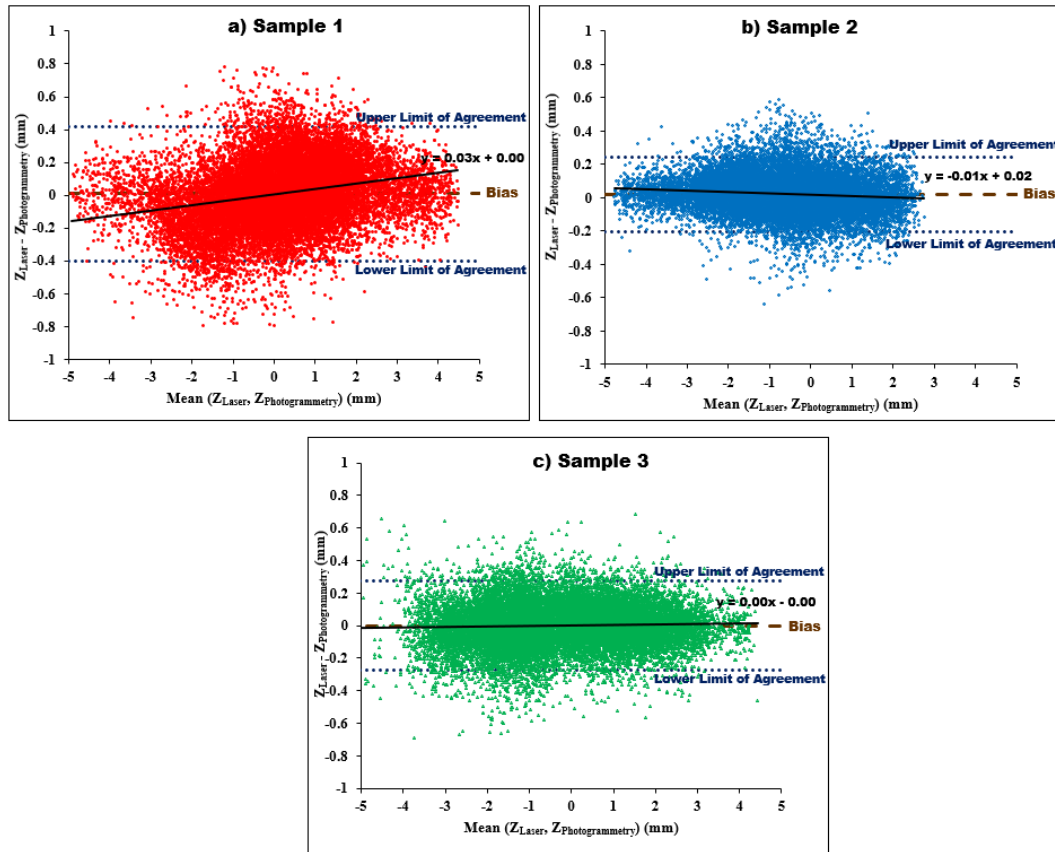


Figure 9. Plot of difference between measurement techniques versus mean of two measurement techniques with 95% limit of agreement for: a) Sample No. 1, b) Sample No. 2, and c) Sample No. 3.

In order to evaluate the dependency of accuracy and preciseness on the joint roughness coefficient (*JRC*) of joint surfaces, the cumulative frequency of measurement differences for all three samples are plotted in Figure 10. The steepness and closeness of the cumulative frequency curve to the vertical axis can be a good representative of prediction precision and accuracy. As noted in Section 3, the *JRC* values for samples No. 1 and No. 2 are similar, while sample No. 3 has the highest *JRC* value. The measurement performance of photogrammetry in sample No. 2 seems better compared to the others. The performance in the roughest joint surface (sample No. 3) is also acceptable and close to that of sample No. 2. Therefore, no obvious dependency of photogrammetry performance on the joint surface roughness is observed, and it seems that the performance is controlled by other parameters.

Several factors control the performance of photogrammetry in the measurement of joint surface characterisations. In terms of systematic errors, they can be sub-divided into the camera and planning factors. The former factors, which result

in image-based errors, are lens distortion, principal distance, and image resolution. The impact of lens distortion and principal distance can be minimized in the camera calibration process by adjusting the relative parameters, as noted in Section 3.2. The image resolution is controlled by the lens focal length, the sensor size, and the camera-to-object distance. The latter factors represent the effect of camera network geometry including baseline distance, ambient light, photograph overlap, angle of incidence, and camera intersection angle [53]. Configuration of the camera and the geometry of the intersecting rays control the propagation of image coordinates error to the corresponding 3-D coordinates [54]. The ambient light can also significantly affect the performance of photogrammetry, where in controlled lighting conditions, the desired features of joint surface can be effectively characterised.

The results from this work show that the photogrammetry method can be a suitable approach for the characterisation of the geometrical texture of joint surfaces. The recent developments in the explicit representation of rock

joint surfaces can lead to a revolutionary advancement in understanding the complex involvement of asperities in the shearing process of rock joints [55-59]. The combined photogrammetry and numerical modelling can provide a powerful tool to develop a more realistic joint roughness parameter that includes both the rock joint geometry and the shearing mechanism. With more accurate modelling of the rock joints using 3D analyses, this methodology can provide a powerful tool for replication of the real geometry of rock joints to understand the complicated shear mechanism of rough rock joints and understand the shear behaviour of large-scale joints, which is recommended for future studies.

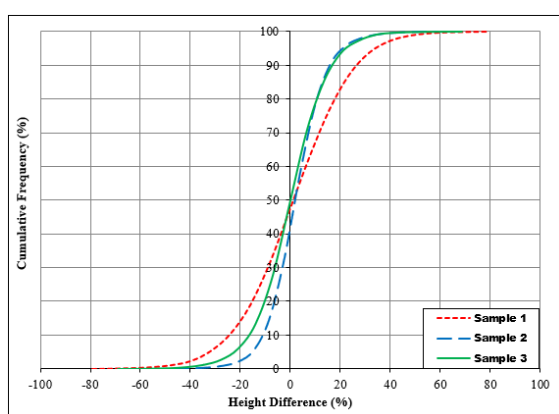


Figure 10. Cumulative frequency of prediction error of samples.

5. Conclusions

The photogrammetry technique has been recognized as an easy and cost-efficient one for creating the geospatial data of large-scale rock slopes, and has been successfully employed to create 3D models of rock structures. However, in terms of the joint roughness investigation, its ability is questionable due to the effects of various factors. The uncertainties in one factor may be associated with the uncertainties in another one. This work investigated the applicability of photogrammetry in the measurement of the micro-scale joint surface texture. In order to study the applicability of photogrammetry for surface roughness characterisation, three tensile joint surfaces were prepared, and the surfaces of these joints were digitized using photogrammetry and a laser scanner with high accuracy ($\pm 50 \mu\text{m}$). A comprehensive statistical analysis was undertaken to investigate whether photogrammetry could be employed to measure the micro-scale texture of rock joints interchangeably with a laser scanner. The results obtained showed that the height

difference distribution of digitized points (between laser scans and photogrammetry) for all three samples followed a normal distribution with the mean value close to zero. The statistical analyses showed that the measured joint surface textures using the photogrammetry technique were in good agreement with the laser scanning results with a good accuracy and an acceptable range of preciseness. It was also found that the accuracy and preciseness of the photogrammetry approach were not dependent on the joint roughness coefficient of the specimens, and camera and planning factors may control the measurement performance.

References

- [1]. Patton, F.D. (1966). Multiple modes of shear failure in rock. Proc, 1st ISRM Congress. Lisbon, Portugal, 509-515.
- [2]. Ladanyi, B. and Archambault, G. (1969). Simulation of shear behavior of a jointed rock mass. Proc, The 11th US Rock Mechanics Symposium (USRMS). Berkeley, CA, 105-125.
- [3]. Ladanyi, B. and Archambault, G. (1980). Direct and indirect determination of shear strength of rock mass. Preprint number 80-25 AIME Annual Meeting. Las Vegas, Nevada 1-16.
- [4]. Barton, N. and Choubey, V. (1977). The shear strength of rock joints in theory and practice. Rock Mechanics, 10 (1-2), 1-54.
- [5]. Grasselli, G. and Egger, P. (2003). Constitutive law for the shear strength of rock joints based on three-dimensional surface parameters. International Journal of Rock Mechanics and Mining Sciences, 40 (1), 25-40.
- [6]. Grasselli, G. (2006). Manuel rocha medal recipient-shear strength of rock joints based on quantified surface description. Rock Mechanics and Rock Engineering, 39 (4), 295-314.
- [7]. Asadollahi, P. and Tonon, F. (2010). Constitutive model for rock fractures: Revisiting Barton's empirical model. Engineering Geology, 113 (1-4), 11-32.
- [8]. Bahaaddini, M. (2017). Effect of Boundary Condition on the Shear Behaviour of Rock Joints in the Direct Shear Test. Rock Mechanics and Rock Engineering, 50 (5), 1141-1155.
- [9]. Bahaaddini, M., Hagan, P., Mitra, R., and Hebblewhite, B.K. (2013). Numerical investigation of asperity degradation in the direct shear test of rock joints. Proc, Eurock 2013 conference. Wroclaw, Poland.
- [10]. Pirzada, M.A., Roshan, H., Sun, H., Oh, J., Andersen, M.S., Hedayat, A. et al. (2020). Effect of contact surface area on frictional behaviour of dry and saturated rock joints. Journal of Structural Geology, 135, 104044.

- [11]. Pirzada, M.A., Bahaaddini, M., Moradian, O., and Roshan, H. (2021). Evolution of contact area and aperture during the shearing process of natural rock fractures. *Engineering Geology*, 291, 106236.
- [12]. Xie, H., Wang, J.-A., and Xie, W.-H. (1997). Fractal effects of surface roughness on the mechanical behavior of rock joints. *Chaos, Solitons and Fractals*, 8 (2), 221-252.
- [13]. Zhang, G., Karakus, M., Tang, H., Ge, Y., and Zhang, L. (2014). A new method estimating the 2D Joint Roughness Coefficient for discontinuity surfaces in rock masses. *International Journal of Rock Mechanics and Mining Sciences*, 72, 191-198.
- [14]. Wang, C., Wang, L., and Karakus, M. (2019). A new spectral analysis method for determining the joint roughness coefficient of rock joints. *International Journal of Rock Mechanics and Mining Sciences*, 113, 72-82.
- [15]. Weissbach, G. (1978). A new method for the determination of the roughness of rock joints in the laboratory. *International Journal of Rock Mechanics and Mining Sciences and Geomechanics Abstracts*, 15 (3), 131-133.
- [16]. Milne, D., Germain, P., and Potvin, Y. (1992). Measurement of rock mass properties for mine design. Proc. ISRM Symposium on Rock Characterization-Eurock 92. London: A.A. Balkema, 245-250.
- [17]. Maerz, N.H., Franklin, J.A., and Bennett, C.P. (1990). Joint roughness measurement using shadow profilometry. *International Journal of Rock Mechanics and Mining Sciences and Geomechanics Abstracts*, 27 (5), 329-343.
- [18]. Maerz, N.H. and Franklin, J.A. (1990). Roughness scale effects and fractal dimension. Proc. First International Workshop on Scale Effects in Rock Masses. Leon, Norway: A.A. Balkema, 121-125.
- [19]. Grasselli, G. (2001). Shear strength of rock joints based on quantified surface description, PhD Thesis, Ecole Polytechnique Fédérale de Lausanne, Switzerland.
- [20]. Thomas, T.R. (1999) *Rough Surfaces*. London: Imperial College Press.
- [21]. Feckers, E. and Rengers, N. (1971). Measurement of large scale roughness of rock planes by means of profilograph and geological compass. Proc. International Symposium on Rock Mechanics. Nancy, France, 1-18.
- [22]. Rasouli, V. and Harrison, J.P. (2004). A comparison of linear profiling and an in-plane method for the analysis of rock surface geometry. *International Journal of Rock Mechanics and Mining Sciences*, 41, Supplement 1 (0), 133-138.
- [23]. Sturzenegger, M. and Stead, D. (2009). Close-range terrestrial digital photogrammetry and terrestrial laser scanning for discontinuity characterization on rock cuts. *Engineering Geology*, 106 (3-4), 163-182.
- [24]. Gaich, A., Potsch, M., and Schubert, W. (2006). Basics and application of 3D imaging systems with conventional and high-resolution cameras. Proc. The 41st US Rock Mechanics Symposium. Alexandria, VA.
- [25]. Propat, G.V. (2006). Remote 3D mapping of rock mass structure. Proc. The 41st US Rock Mechanics Symposium. Alexandria, VA.
- [26]. Tonon, F. and Kottenstette, J.T. (2006). Laser and photogrammetric methods for rock face characterization. Proc. The 41st US Rock Mechanics Symposium. Alexandria, VA.
- [27]. Birch, J.S. (2006). Using 3DM Analyst Mine Mapping Suite for rock face characterization. Proc. The 41st US Rock Mechanics Symposium. Alexandria, VA.
- [28]. Zhang, D., Zhang, Y., Cheng, T., Meng, Y., Fang, K., Garg, A. *et al.* (2017). Measurement of displacement for open pit to underground mining transition using digital photogrammetry. *Measurement*, 109, 187-199.
- [29]. Firpo, G., Salvini, R., Francioni, M., and Ranjith, P.G. (2011). Use of digital terrestrial photogrammetry in rocky slope stability analysis by distinct elements numerical methods. *International Journal of Rock Mechanics and Mining Sciences*, 48 (7), 1045-1054.
- [30]. Voyat, I., Roncella, R., Forlani, G., and Ferrero, A.M. (2006). Advanced techniques for geo structural surveys in modelling fractured rock masses: application to two Alpine sites. Proc. The 41st US Rock Mechanics Symposium. Alexandria, VA.
- [31]. Tannant, D.D. (2015). Review of photogrammetry-based techniques for characterization and hazard assessment of rock faces *International Journal of Geohazards and Environment*, 1 (2), 76-87.
- [32]. Haneberg, W. (2008). Using close range terrestrial digital photogrammetry for 3-D rock slope modeling and discontinuity mapping in the United States. *Bulletin of Engineering Geology and the Environment*, 67 (4), 457-469.
- [33]. Kottenstette, J.T. (2005). Measurement of geologic features using close range terrestrial photogrammetry. Proc. The 40th US Symposium on Rock Mechanics. Anchorage, Alaska, USA.
- [34]. Tonon, F. and Kottenstette, J.T. (2006). Summary paper on the Morrison field exercise. Proc. The 41st US Rock Mechanics Symposium. Alexandria, VA.
- [35]. Gaich, A. and Pötsch, M. (2016). Gaich 2016 3D images for digital tunnel face documentation at TBM headings – Application at Koralmtunnel lot KAT2 *Geomechanics and Tunneling*, 9 (3), 210-221.
- [36]. Niedostatkiewicz, M., Lesniewska, D., and Tejchman, J. (2011). Experimental analysis of shear zone patterns in cohesionless for earth pressure

problems using particle image velocimetry, *Strain*, 47: 218-231.

[37]. Khosravi, M.H., Pipatpongsa, T., and Takemura, J. (2013). Experimental analysis of earth pressure against rigid retaining walls under translation mode. *Geotechnique*, 63 (12), 1020-1028.

[38]. Ganiyu, A.A., Rashid, A.S.A., and Osman, M.H. (2016). Utilization of transparent synthetic soil surrogates in geotechnical physical models: A review. *Journal of Rock Mechanics and Geotechnical Engineering*, 8 (4), 568-576.

[39]. Khosravi, M.H., Pipatpongsa, T., Takahashi, A., and Takemura, J. (2011). Arch action over an excavated pit on a stable scarp investigated by physical model tests. *Soils and Foundations*, 51 (4), 723-735.

[40]. Khosravi, M., Tang, L., Pipatpongsa, T., Takemura, J., and Doncommul, P. (2012). Performance of counterweight balance on stability of undercut slope evaluated by physical modeling. *International Journal of Geotechnical Engineering*, 6 (2), 193-205.

[41]. Masoumi, H. (2013). Investigation into the mechanical behaviour of intact rock at different sizes PhD Thesis, UNSW Australia, Sydney.

[42]. Masoumi, H., Bahaaddini, M., Kim, G., and Hagan, P. (2014). Experimental investigation into the mechanical behavior of Gosford sandstone at different sizes. *Proc. 48th US Rock Mechanics/Geomechanics Symposium: American Rock Mechanics Association*.

[43]. Bahaaddini, M., Serati, M., Masoumi, H., and Rahimi, E. (2019). Numerical assessment of rupture mechanisms in Brazilian test of brittle materials. *International Journal of Solids and Structures*, 180-181, 1-12.

[44]. Lv, A., Masoumi, H., Walsh, S.D.C., and Roshan, H. (2019). Elastic-softening-plasticity around a borehole: an analytical and experimental study. *Rock Mechanics and Rock Engineering*, 52 (4), 1149-1164.

[45]. Myers, N.O. (1962). Characterization of surface roughness. *Wear*, 5 (3), 182-189.

[46]. Tse, R. and Cruden, D.M. (1979). Estimating joint roughness coefficients. *International Journal of Rock Mechanics and Mining Sciences and Geomechanics Abstracts*, 16 (5), 303-307.

[47]. ADAM Technology. (2010) 3DM analyst mine mapping suite manual. Perth, Australia

[48]. Bahaaddini, M. and Hosseinpour Moghadam, E. (2019). Evaluation of empirical approaches in estimating the deformation modulus of rock masses, *Bulletin of Engineering Geology and the Environment*, 78 (5), 3493-3507.

[49]. Bland, J.M. and Altman, D.G. (1995). Comparing methods of measurement: why plotting difference against standard method is misleading. *Lancet* (London, England), 346 (8982), 1085-1087.

[50]. Bland, J.M. and Altman, D.G. (1986). Statistical methods for assessing agreement between two methods of clinical measurement. *Lancet* (London, England), 1 (8476), 307-310.

[51]. Bland, J.M. and Altman, D.G. (1999). Measuring agreement in method comparison studies. *Statistical methods in medical research*, 8 (2), 135-160.

[52]. Montenij, L.J., Buhre, W.F., Jansen, J.R., Kruitwagen, C.L., and de Waal, E.E. (2016). Methodology of method comparison studies evaluating the validity of cardiac output monitors: a stepwise approach and checklist. *British Journal of Anaesthesia*, 116 (6), 750-758.

[53]. Kim, D.H., Poropat, G., Gratchev, I., and Balasubramaniam, A. (2016). Assessment of the accuracy of close distance photogrammetric JRC data. *Rock Mechanics and Rock Engineering*, 49 (11), 4285-4301.

[54]. El-Hakim, S.F., Beraldin, J.A., and Blais, F. (1995) Comparative evaluation of the performance of passive and active 3D vision systems, *Proc. SPIE 2646, Digital Photogrammetry and Remote Sensing*.

[55]. Bahaaddini, M., Hagan, P.C., Mitra, R., and Khosravi, M.H. (2016). Experimental and numerical study of asperity degradation in the direct shear test. *Engineering Geology*, 204, 41-52.

[56]. Bahaaddini, M., Hagan, P.C., Mitra, R., and Hebblewhite, B.K. (2015). Parametric study of smooth joint parameters on the shear behaviour of rock joints. *Rock Mechanics and Rock Engineering*, 48 (3), 923-940.

[57]. Asadi, M., Rasouli, V., and Barla, G. (2012). A bonded particle model simulation of shear strength and asperity degradation for rough rock fractures. *Rock Mechanics and Rock Engineering*, 45 (5), 649-675.

[58]. Bahaaddini, M., Sharrock, G., Hebblewhite, B., and Mitra, R. (2012). Direct shear tests to model the shear behaviour of rock joints by PFC2D. 46th US Rock Mechanics/Geomechanics Symposium. Chicago, IL, USA: American Rock Mechanics Association.

[59]. Bahaaddini, M. (2014). Numerical study of the mechanical behaviour of rock joints and non-persistent jointed rock masses, PhD Thesis, UNSW Australia, Sydney, Australia.

توصیف زبری کوچک مقیاس سطح درزه سنگی با استفاده از روش فتوگرامتری

مجتبی بهالدینی^{۱*}، مهدی صراطی^۲، محمد حسین خسروی^۱ و بروس هبلوایت^۴

- ۱- دانشکده مهندسی معدن، دانشکدگان فنی، دانشگاه تهران، تهران، ایران
 ۲- بخش مهندسی معدن، دانشگاه شهید باهنر کرمان، کرمان، ایران
 ۳- دانشکده مهندسی عمران، دانشگاه کوینزلند، بریزبن، استرالیا
 ۴- دانشکده مهندسی مواد معدنی و منابع انرژی، دانشگاه نیوساوت ولز، سیدنی، استرالیا

ارسال ۲۰۲۲/۰۲/۱۵، پذیرش ۲۰۲۲/۰۲/۲۸

* نویسنده مسئول مکاتبات: m.bahaaddini@ut.ac.ir

چکیده:

درک صحیح از رفتار برشی درزه‌های سنگی و ناپیوستگی‌ها همواره به عنوان یک چالش در تحقیقات مهندسی مکانیک سنگ شناخته می‌شود و این چالش بدلیل مشکلات متعددی در توصیف کمی زبری سطح درزه، چه در مقیاس برجا و چه در مقیاس آزمایشگاهی می‌باشد. تجهیزات و روش‌های متعددی در سال‌های اخیر برای توصیف سطح درزه‌ها در مطالعات آزمایشگاهی و برجا توسعه پیدا کرده است که در میان این روش‌ها، فتوگرامتری دارای مقبولیتی روزافزون می‌باشد. در این تحقیق به بررسی توانایی روش فتوگرامتری در توصیف توپوگرافی سطح درزه و ساختار آن در کوچک مقیاس پرداخته می‌شود. برای این منظور، سه سطح درزه سنگی نوع کشتی با استفاده روش فتوگرامتری رقومی شده و نتایج آن نتایج اسکن لیزری سه بعدی با دقت بالا مقایسه می‌شود. سپس جهت ارزیابی توانایی روش فتوگرامتری در توصیف سطوح درزه، آنالیز آماری جامعی بر روی ابر نقاط رقومی شده انجام می‌شود. نتایج این بررسی نشان می‌دهد که اختلاف ارتفاع بین ابر نقاط منتج شده از دو روش فتوگرامتری و اسکن لیزری سه بعدی، از توزیع آماری نرمال با مقدار متوسط نزدیک به صفر تبعیت می‌کند. تحلیل‌های آماری نشان می‌دهد که سطوح برداشت شده در روش فتوگرامتری انطباق مناسبی با داده‌های اسکن لیزری داشته و توانایی روش فتوگرامتری در توصیف سطح درزه حتی در کوچک مقیاس را تایید می‌نماید. همچنین نتایج این بررسی نشان می‌دهد که دقت و صحت روش فتوگرامتری مستقل از ضریب زبری سطح درزه بوده، اما پارامترهای دوربین و شرایط محیطی می‌تواند عملکرد برداشت را بطور قابل ملاحظه‌ای تحت تاثیر قرار دهند.

کلمات کلیدی: درزه سنگی، زبری سطح درزه، رفتار برشی، فتوگرامتری، اسکن لیزری.